Cement and Concrete Research 40 (2010) 699–709

Contents lists available at ScienceDirect

Cement and Concrete Research

journal homepage: http://ees.elsevier.com/CEMCON/default.asp

Experimental determination of the thermodynamic parameters affecting the adsorption behaviour and dispersion effectiveness of PCE superplasticizers

J. Plank *, B. Sachsenhauser, J. de Reese

Chair for Construction Chemicals, Technische Universität München, 85747 Garching, Germany

ARTICLE INFO

Article history:
Received 13 May 2009
Accepted 7 December 2009

Keywords:
Adsorption (C)
Polycarboxylates
$CaCO_3$ (D)
Thermodynamic calculations (B)
Workability (A)

ABSTRACT

For adsorption of three different allylether-based PCE superplasticizers on $CaCO_3$ surface, the thermodynamic parameters ΔH, ΔS and ΔG were determined experimentally. The GIBBS standard free energy of adsorption ΔG_{0ads}, the standard enthalpy of adsorption ΔH_{0ads} and the standard entropy of adsorption ΔS_{0ads} applying to an unoccupied $CaCO_3$ surface were obtained via a linear regression of ln K (equilibrium constant) versus $1/T$ (VAN'T HOFF plot). Additionally, the thermodynamic parameters characteristic for a $CaCO_3$ surface loaded already with polymer (isosteric conditions) were determined using a modified CLAUSIUS–CLAPEYRON equation.

For all PCE molecules, negative ΔG values were found, indicating that adsorption of these polymers is energetically favourable and a spontaneous process. Adsorption of PCEs possessing short side chains is mainly instigated by electrostatic attraction and a release of enthalpy. Contrary to this, adsorption of PCEs with long side chains occurs because of a huge gain in entropy. The gain in entropy results from the release of counter ions attached to the carboxylate groups of the polymer backbone and of water molecules and ions adsorbed on the $CaCO_3$ surface. With increased surface loading, however, $\Delta G_{isosteric}$ decreases and adsorption ceases when ΔG becomes 0. The presence of Ca^{2+} ions in the pore solution strongly impacts PCE adsorption, due to complexation of carboxylate groups and a reduced anionic charge amount of the molecule. In the presence of Ca^{2+}, adsorption of allylether-based PCEs is almost exclusively driven by a gain in entropy. Consequently, PCEs should produce a strong entropic effect upon adsorption to be effective cement dispersants. Molecular architecture, anionic charge density and molecular weight as well as the type of anchor groups present in a superplasticizer determine whether enthalpy or entropy is the dominant force for superplasticizer adsorption.

1. Introduction

Adsorption of PCEs on a $CaCO_3$ surface is an exergonic process if the GIBBS free energy of adsorption is negative in sign. According to the GIBBS–HELMHOLTZ equation (Eq. (1)), this occurs if heat is released ($\Delta H<0$) and/or the entropy of the entire system increases ($\Delta S>0$) as a result of adsorption.

$$\Delta G = \Delta H - T \cdot \Delta S \tag{1}$$

Generally, the adsorption of polyelectrolytes on oppositely charged surfaces results from the sum of four energy contributions [1]. The first one derives from the attraction energy between charged or partially coordinated atoms present on the mineral surface and the oppositely charged polyelectrolyte. The second term describes segment–segment repulsion resulting from the electrostatic repulsion between adsorbed segments bearing the same electrostatic charge. The third term expresses the loss of entropy owed to a decreased conformational flexibility of the adsorbed polymer once the segments of the trunk chain become fixed to the surface. The fourth term presents the gain in entropy accompanying the release of a large number of counter ions into the bulk solution when the polyelectrolyte is adsorbed through an ion-exchange mechanism. The first and the fourth of these contributions favour adsorption while the second and the third one work against it. Consequently, adsorption occurs only if the positive contributions exceed the hindering forces.

Determination of the adsorption isotherms at different temperatures allows plotting a linear LANGMUIR regression from which according to Eq. (2), the equilibrium constant K between non-adsorbed and adsorbed polymer at a given temperature can be calculated [1].

$$\frac{C_{eq}}{Q_{ads}} = \frac{C_{eq}}{Q_{max}} + \frac{1}{K \cdot Q_{max}} \tag{2}$$

C_{eq} corresponds to the equilibrium concentration of the polymer in solution in mol/L, Q_{ads} is the adsorbed amount of PCE in mol/g at a

* Corresponding author. TU München, Lehrstuhl für Bauchemie, Lichtenbergstr. 4, 85747 Garching, Germany. Tel.: +49 89 289 13150.
E-mail address: sekretariat@bauchemie.ch.tum.de (J. Plank).

0008-8846/$ – see front matter © 2010 Elsevier Ltd. All rights reserved.
doi:10.1016/j.cemconres.2009.12.002

given polymer dosage, Q_{max} is the maximum adsorbed amount of PCE at the point of saturation, and K is the temperature dependent equilibrium constant. A plot of C_{eq}/Q_{max} versus C_{eq} produces a straight line. From the slope and the intercept point with the y-axis of this linear regression, the equilibrium constant K can be calculated. The temperature dependence of K is described by the VAN'T HOFF equation (Eq. (3)). By plotting ln K versus $1/T$, the standard enthalpy of adsorption ΔH_0 can be obtained from the slope and the standard entropy of adsorption ΔS_0 from the intercept point of the line with the y-axis. Using these values for ΔH_0 and ΔS_0, the GIBBS free energy of adsorption ΔG_0 can be calculated using the GIBBS–HELMHOLTZ equation.

$$\ln K = \frac{\Delta S_0}{R} - \frac{\Delta H_0}{R \cdot T} \tag{3}$$

whereby R is the universal gas constant (8.314 J/mol K).

The thermodynamic calculations based on the linear LANGMUIR and VAN'T HOFF plots do not consider the influence on the adsorption process owed to increasing surface coverage of the substrate by PCE. Thus, the values determined for ΔH_0, ΔS_0 und ΔG_0 only represent the ideal case of an unoccupied and homogeneous surface, i.e. they describe the forces at the beginning of the adsorption process. In that way, they represent only a rough approximation [2]. Surface coverage-dependent free energy, enthalpy and entropy of adsorption can be determined by using a modified CLAUSIUS–CLAPEYRON equation (Eq. (4)) [3]. There, $C_{eq(isosteric)}$ is the concentration of polymer in solution at a constant surface coverage. $C_{eq(isosteric)}$ can be obtained from the adsorption isotherm by the use of a polynomial approximation. The linear regression of ln $C_{eq(isosteric)}$ versus $1/T$ at a specific, constant surface coverage produces a straight line. From the slope of the line, the isosteric enthalpy of adsorption $\Delta H_{(isosteric)}$ and from the intercept point with the y-axis, the isosteric entropy of adsorption $\Delta S_{(isosteric)}$ can be calculated. This way, the thermodynamic parameters of the adsorption process can be examined at different surface loadings of the substrate with PCE.

$$\frac{\Delta H_{(isosteric)}}{R} = \frac{\ln[C_{eq(isosteric)}]}{1/T} \tag{4}$$

In cement pore solution, limestone exhibits a positive surface charge. This charge correlates with that of several hydration products of cement, such as ettringite (AF_t) or monosulfoaluminate (AF_m) [6]. For this reason, limestone represents a suitable model substrate to investigate the adsorption process of polycarboxylates on positively charged cement hydrate phases. However, the pore solutions of limestone and cement suspensions are quite different with respect to their pH value and ionic composition. Cement pore solution shows a strongly alkaline pH value (pH=12.5–13.5), a high concentration of electrolytes (~20–30 g salts/L) and, consequently, a higher ionic strength than a $CaCO_3$ suspension. Amongst other ions, it contains up to 1 g/L of solved Ca^{2+} ions. pH, ionic strength and concentration of solved Ca^{2+} ions, however, have a major impact on the quantity of superplasticizer which adsorbs onto the surface of inorganic particles. At the same time, the adsorbed amount is an important parameter which greatly impacts the dispersing effectiveness of a superplasticizer. Dispersion is achieved via electrostatic repulsion or the steric hindrance mechanism of adsorbed graft chains [4,5,7].

In this study, the thermodynamic parameters ΔG, ΔH and ΔS for the adsorption of allylether-based PCE superplasticizers on aqueous suspensions of limestone were determined experimentally. To simulate the conditions occurring in cement pore solution, the liquid phase of the limestone suspension (pH 9; 20 mg/L Ca^{2+} at w/$CaCO_3$ 0.425) was loaded stepwise with electrolytes at concentrations which exist in cement pore solution. This step was made to obtain results which better describe PCE adsorption behaviour in cement paste. In such saline environment, the anionic charge of the polymer and the surface charge of limestone will be different from that existing in a native $CaCO_3$ suspension.

The thermodynamic parameters ΔG, ΔH and ΔS for the adsorption process of PCEs onto the $CaCO_3$ surface as it exists in strongly alkaline, Ca^{2+} loaded suspension were determined via temperature dependent adsorption measurements. Additionally, the impact of pH and Ca^{2+} concentration present in the pore solution on the surface charge of the substrate and the anionic charge density of the PCEs were examined. This way, it was possible to assess the electrostatic contribution to PCE adsorption and its impact on the amount of PCE adsorbed onto the mineral surface.

2. Materials and methods

2.1. Polycarboxylates

Three polycarboxylates possessing different molecular architectures based on α-allyl-ω-methoxy polyethylene glycol-maleic anhydride copolymers were synthesized via bulk radical copolymerisation of maleic anhydride with an allylether macromonomer at a molar ratio of 1:1. Their general chemical structure is presented in Fig. 1. The copolymers show an alternating monomer sequence (A–B–A–B type) because allylether monomers do not homopolymerize. Details of the synthesis process have been described before [7].

All PCEs were dialysed for two days using an 8000 Da cut off Spectra/Por cellulose membrane (Spectrum Laboratories Inc., Rancho Dominguez, USA). The synthesized allylether copolymers were characterized by aqueous GPC using a 2695 GPC separation module (Waters, Eschborn, Germany) containing a 2414 RI detector (Waters, Eschborn, Germany) and a Dawn EOS 3 angle light scattering detector (Wyatt Technology, Clinton IA/USA). Ultrahydrogel columns 500, 250, and 120 (Waters, Eschborn, Germany) with an operating range (PEO/PEG) of M_w = 100 to 1,000,000 Da were used. Eluent was 0.1 N $NaNO_3$ with pH 12 adjusted by NaOH.

2.2. Anionic charge density of PCEs

Anionic charge densities of the PCEs were measured in filtrates obtained from the limestone suspension at pH 9, pH 12.6 and pH 12.6 plus 3.675 g/L $CaCl_2 \cdot 2H_2O$ (this corresponds to a Ca^{2+} concentration of 1 g/L). Charge titration was performed using a Mütek PCD 03 pH titrator (Mütek, Herrsching, Germany) and Poly-DADMAC as the cationic counter polymer. Details of the experimental procedure have been described before [8]. Here, 10 mL of the 0.2 g/L PCE solution were filled into the measuring cell and titrated in 0.1 mL steps with aqueous Poly-DADMAC (Mütek, Herrsching, Germany). From the consumption of cationic polyelectrolyte needed to neutralize the anionic charge of the polymer, the anionic charge density of the PCEs can be calculated.

2.3. Limestone

Limestone powder Precal 18 (Schäfer, Diez, Germany) with a density of 2.74 g/cm^3 and an average particle size (d_{50}) of 9.71 µm was

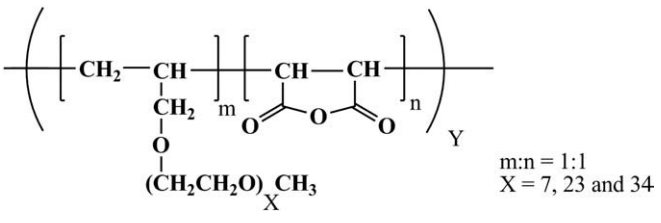

Fig. 1. Chemical structure of the synthesized allylether-maleic anhydride copolymers.

used for all experiments. Its purity was 98.5% calcite (QXRD). The specific surface area (BET, N_2) was found to be 0.488 m^2/g.

All experiments with limestone suspension were performed at a w/$CaCO_3$ ratio of 0.425. When suspended in DI water, this $CaCO_3$ suspension shows a pH of 9.

2.4. Adsorption

PCE adsorption on $CaCO_3$ was measured according to the depletion method. The non-adsorbed portion of PCE remaining in solution at equilibrium condition was determined by measuring the total organic content (TOC) of the solution. Adsorption was measured for three different suspensions using DI water (pH 9), NaOH solution (pH 12.6), and NaOH solution (pH 12.6) containing 3.675 g/L $CaCl_2 \cdot 2H_2O$ (1 g/L Ca^{2+}) as solvent. In a typical experiment, 16 g of $CaCO_3$ and 6.8 mL of PCE solution (concentration 0.2–6 g/L) were filled separately into 50 mL centrifuge glasses and stored for 24 h in a drying oven at room temperature, 40 °C and 60 °C, resp. The preconditioned samples were then combined by adding the limestone powder to the PCE solution. The resulting suspension was shaken in a wobbler at 2400 rpm (VWR International, Darmstadt, Germany) for 2 min and then centrifuged at the respective temperature for 10 min at 8500 rpm. The supernatant was diluted with deionised water. The total organic carbon of the solution was determined by combustion at 890 °C on a HIGH TOC II (Elementar, Hanau, Germany). To obtain the carbon content in the PCE solutions, the same PCE solutions without addition of $CaCO_3$ were taken and measured in the same manner. From the difference between the TOC content of the PCE reference sample and the TOC content of the supernatant of the $CaCO_3$ suspension, the adsorbed amount of PCE was calculated. Measurements were generally repeated three times and the average as well as the range of individual values obtained in each test is displayed by respective points and bars in the adsorption isotherms. All parameters derived from these values by calculation show a similar error estimation.

2.5. Zeta potential

Zeta potentials were determined with Model DT-1200 Electroacoustic Spectrometer (Dispersion Technology Inc., New York). This instrument was chosen because it allows to measure zeta potentials of highly solids loaded liquids. The zeta potential of the $CaCO_3$ suspension was measured as follows: Within 1 min, 350 g of limestone meal were added to 148.75 mL of either DI water, of aqueous NaOH (pH 12.6) or aqueous NaOH (pH 12.6) loaded with 1 g/L Ca^{2+}. The suspension was stirred for 2 min before the measurement was taken.

Additionally, the zeta potential of a $CaCO_3$ suspension in DI water (pH 9) was measured under stepwise titration of an aqueous solution of PCE sample S7-M31 (concentration: 2 M.-%) until a polymer dosage of 0.2 M.-% bwo$CaCO_3$ was reached. The total time for the titration was 1 h.

3. Results

3.1. Properties of the PCE samples

The characteristic data of the copolymers are listed in Table 1. For the polymers, the designation *SX-MY* was used. *X* describes the number of ethylene oxide units per side chain (*S*) and *Y* presents the number of repeating units in the trunk chain (*M*). Consequently, *Y* describes the main chain length and also specifies the number of side chains per macromolecule (see Fig. 1). *Y* was calculated from M_n obtained from GPC by using a method described in an earlier publication [7,9].

Table 1
Molar masses (M_w and M_n), polydispersity index (PDI), purity of polymer, number of ethylene oxide units per side chain (*X*) and total number (average) of side chains per macromolecule (*Y*) for synthesized PCEs.

PCE polymer	M_w [Da]	M_n [Da]	PDI M_w/M_n	Polymer content [M.-%]	*X* n_{EO}	*Y*
S7-M31	37,030	15,310	2.4	94.0	7	31.1
S23-M19	103,200	22,370	4.6	94.6	23	18.7
S34-M13	60,530	21,290	2.8	74.2	34	12.7

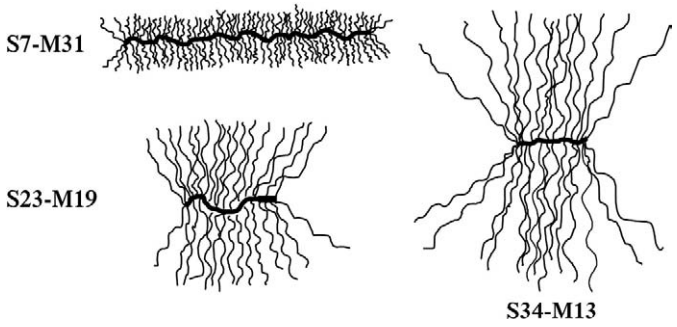

Fig. 2. Schematic illustration of the molecular architecture and size to scale of the synthesized allylether PCEs.

The synthesized PCEs differ with respect to their molecular architecture and size. Fig. 2 shows a schematic representation to scale of the macromolecules. The polymers differ in their ratio between trunk and side chain length. In S7-M31, the trunk chain is about seven times longer than a side chain. It represents a brush or worm polymer. In S34-M13, however, the side chains are much longer than the trunk chain, giving it the shape of a star polymer.

In plain $CaCO_3$ suspension, the anionic charge densities of the PCE molecules were found to decrease with increasing side chain length from 1845 to 526 μeq/g (Table 2). This behaviour is explained by the decreasing amount of negatively charged carboxylate groups per mass of the polymer when the side chain becomes longer. At higher pH values of the pore solution, the anionic charge density of the PCEs increased to values between 1004 and 3272 μeq/g. This effect is owed to increased deprotonation of the carboxylate groups in the polymer backbone at higher pH. In the presence of Ca^{2+} ions, however, the anionic charge density of the PCEs decreased strongly to values of between 0 and 262 μeq/g. The reason for this effect is complexation of carboxylate groups with Ca^{2+} ions [8,10]. This observation is particularly important when studying PCEs in cementitious systems. There, the Ca^{2+} concentration in pore solution is relatively high (1 g/L Ca^{2+}) and constantly fed by dissolution of clinker phases.

From the results shown in Table 2 it can be concluded that, in Ca^{2+} loaded pore solutions, these PCEs possess very low anionic charge densities. Consequently, electrostatic attraction between these PCEs and a positively charged surface should be low.

3.2. Zeta potential of the $CaCO_3$ suspension

The zeta potential of $CaCO_3$ particles suspended in different pore solutions is shown in Table 3. In water at pH 9, the zeta potential of

Table 2
Specific anionic charge densities of the synthesized PCEs measured in different pore solutions containing suspended limestone (w/$CaCO_3$ = 0.425).

Type of pore solution	PCE polymer	Specific anionic charge density [μeq/g]
water @ pH 9	S7-M31	1845
water @ pH 9	S23-M19	747
water @ pH 9	S34-M13	526
water @ pH 12.6	S7-M31	3272
water @ pH 12.6	S23-M19	1543
water @ pH 12.6	S34-M13	1004
water @ pH 12.6 plus 1 g/L Ca^{2+}	S7-M31	262
water @ pH 12.6 plus 1 g/L Ca^{2+}	S23-M19	194
water @ pH 12.6 plus 1 g/L Ca^{2+}	S34-M13	0

Table 3
Zeta potential of $CaCO_3$ suspended in different pore solutions (w/$CaCO_3$ = 0.425).

Type of pore solution	Zeta potential [mV]
water @ pH 9	+20
water @ pH 12.6	−12
water @ pH 12.6 plus 1 g/L Ca^{2+}	+36

$CaCO_3$ is positive, whereas at pH 12.6 it becomes negative in sign. The isoelectric point was found to be at pH 11. In the presence of 1 g/L Ca^{2+} ions at pH 12.6, however, the zeta potential of $CaCO_3$ becomes highly positive again (+36 mV). This effect is due to the adsorption of Ca^{2+} ions onto the negatively charged $CaCO_3$ surface.

It can be concluded that the surface charge of $CaCO_3$ is strongly affected by the pH and the presence of multivalent ions such as e.g. Ca^{2+} present in the pore solution. In cement pore solution, $CaCO_3$ can develop a highly positive surface charge similar to that of several cement hydrate phases. Therefore, $CaCO_3$ is a suitable model substrate to study the adsorption behaviour of PCE superplasticizers on the surfaces of cement hydrates.

In the next step, the thermodynamic parameters ΔG, ΔH and ΔS characteristic for the adsorption of different PCEs on $CaCO_3$ possessing different surface charges were determined. It was particularly interesting to study whether these different surface charges of $CaCO_3$ will have an impact on the adsorbed amounts of PCE and the thermodynamic parameters.

3.3. Determination of thermodynamic parameters

Next, the standard enthalpy of adsorption ΔH_0, the standard entropy of adsorption ΔS_0 and the GIBBS free energy of adsorption ΔG_0 were determined from the adsorption isotherms measured at RT (21.5 °C), 40 °C and 60 °C, resp.

The adsorption isotherms for each PCE polymer in the three different pore solutions are shown in Figs. 3–11. For each condition, three independent measurements were taken. The average is indicated as a point and the range of values obtained is shown as a bar in the isotherms displayed in Figs. 3–11. Where no bar is visible in the graph, the error was too small to show. Generally, the margin of error was less than ±5%, except for polymer PCE S7-M31 which consistently showed a tendency to higher deviation, particularly at 60 °C (up to ±12.5%). The reason for this effect remained unknown.

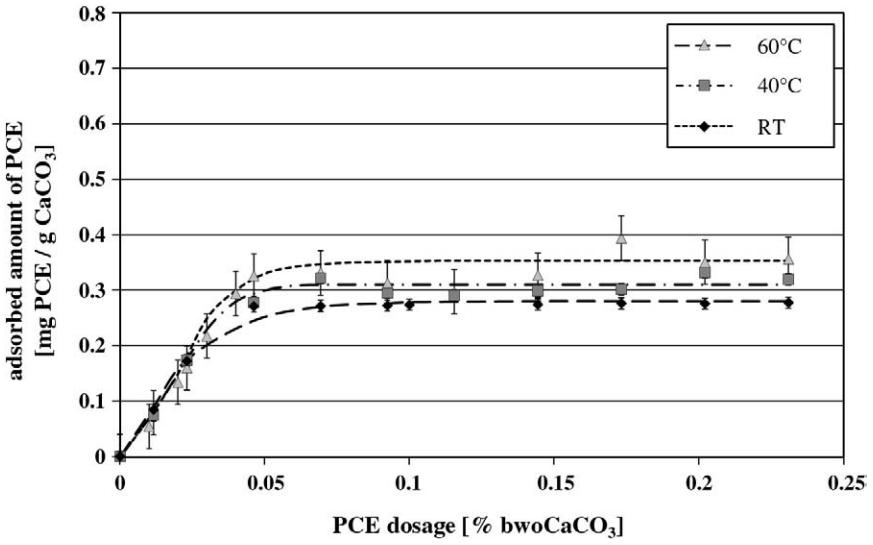

Fig. 3. Adsorption isotherms for PCE S7-M31 on $CaCO_3$ at pH 9 and RT, 40 °C and 60 °C, resp.

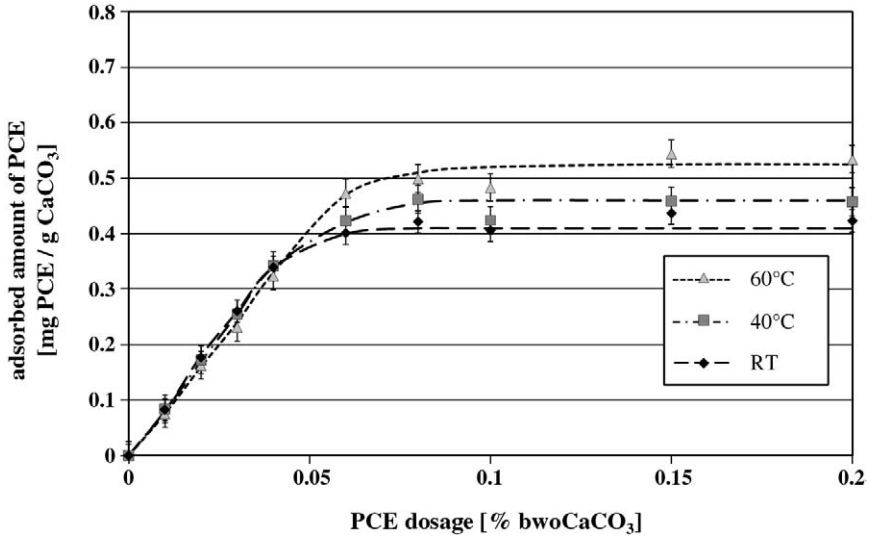

Fig. 4. Adsorption isotherms for PCE S23-M19 on $CaCO_3$ at pH 9 and RT, 40 °C and 60 °C, resp.

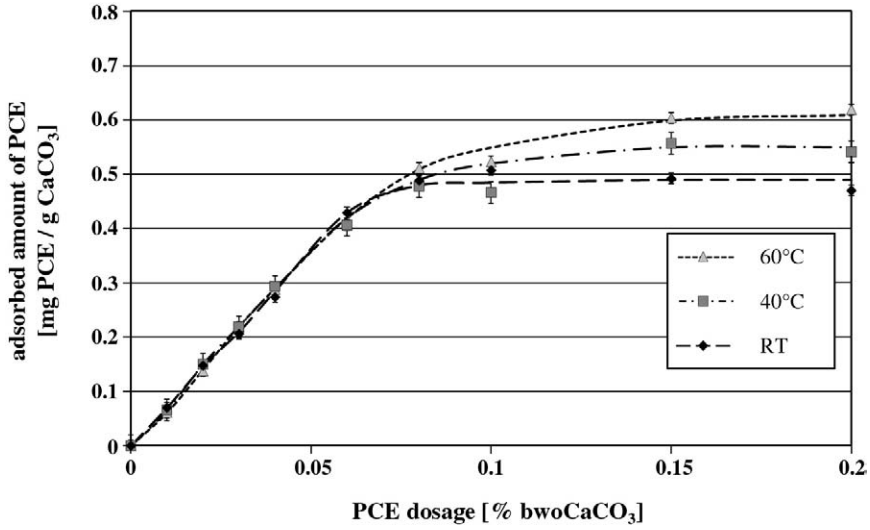

Fig. 5. Adsorption isotherms for PCE S34-M13 on $CaCO_3$ at pH 9 and RT, 40 °C and 60 °C, resp.

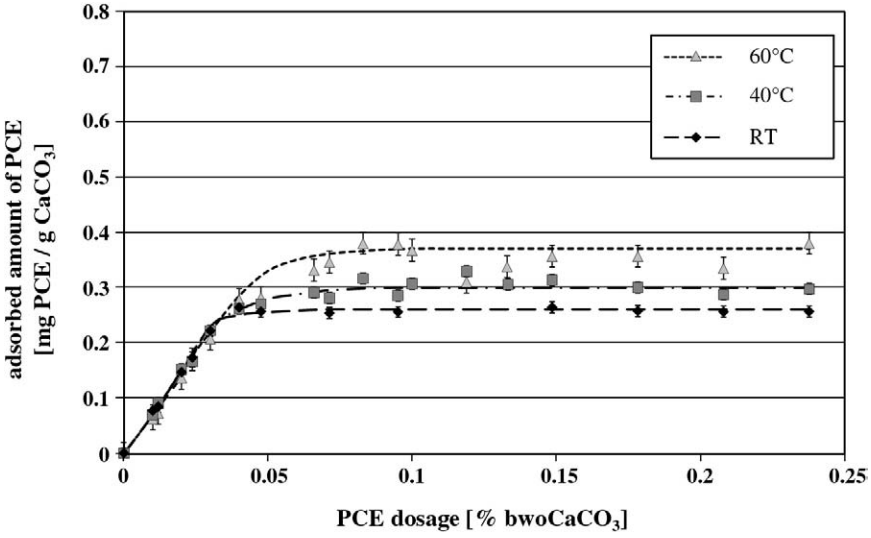

Fig. 6. Adsorption isotherms for PCE S7-M31 on $CaCO_3$ at pH 12.6 and RT, 40 °C and 60 °C, resp.

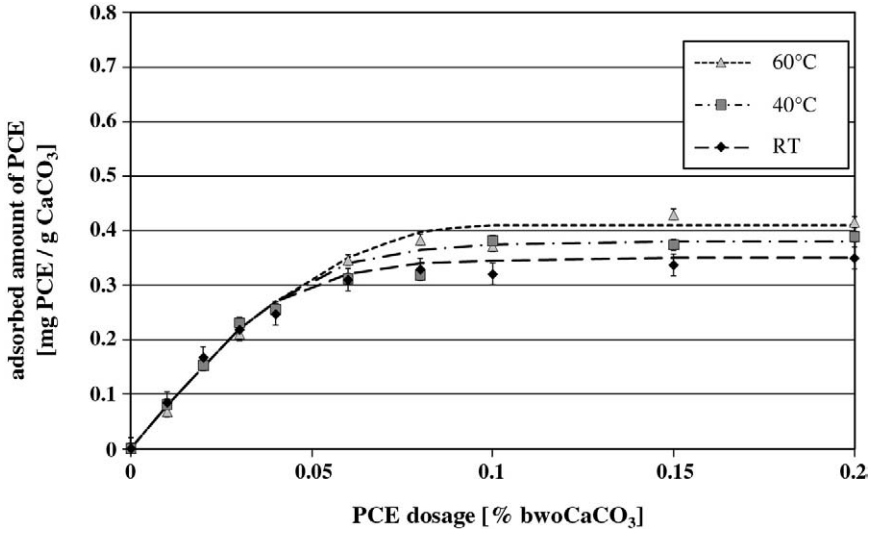

Fig. 7. Adsorption isotherms for PCE S23-M19 on $CaCO_3$ at pH 12.6 and RT, 40 °C and 60 °C, resp.

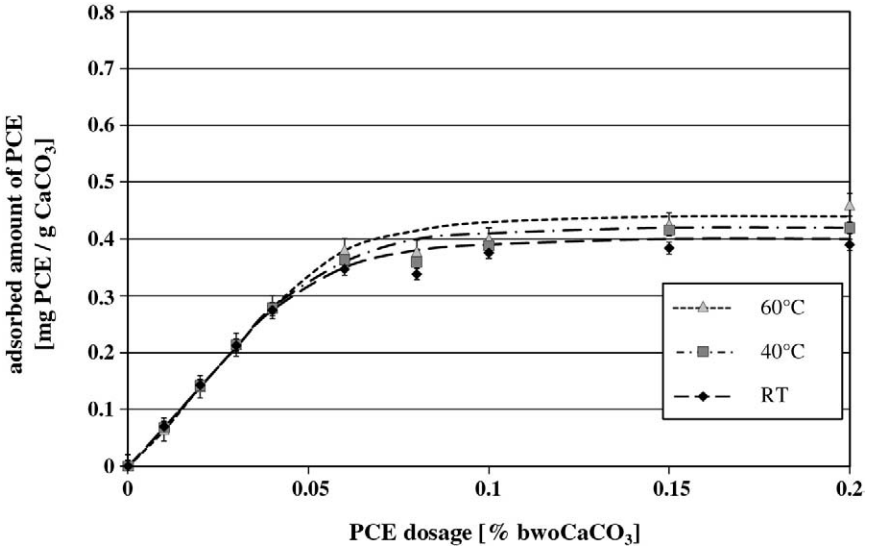

Fig. 8. Adsorption isotherms for PCE S34-M13 on $CaCO_3$ at pH 12.6 and RT, 40 °C and 60 °C, resp.

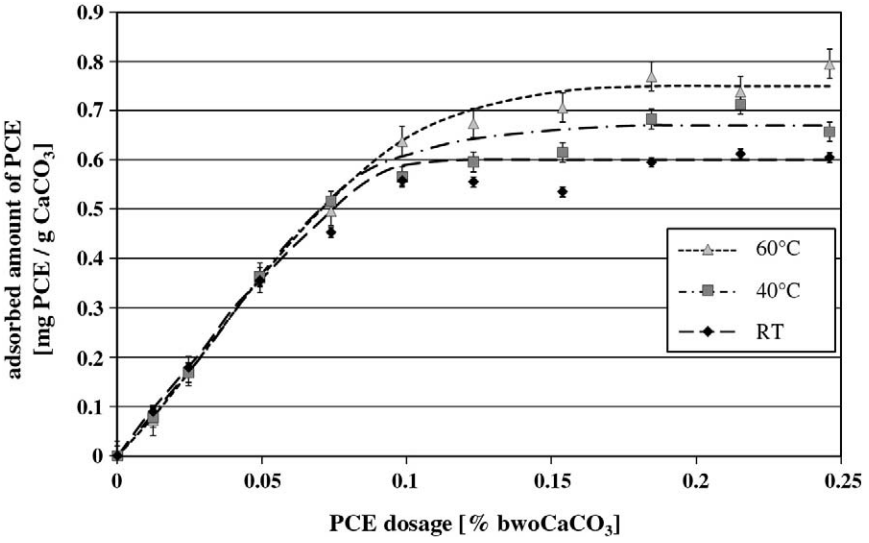

Fig. 9. Adsorption isotherms for PCE S7-M31 on $CaCO_3$ at pH 12.6 + 1 g/L Ca^{2+} and RT, 40 °C and 60 °C, resp.

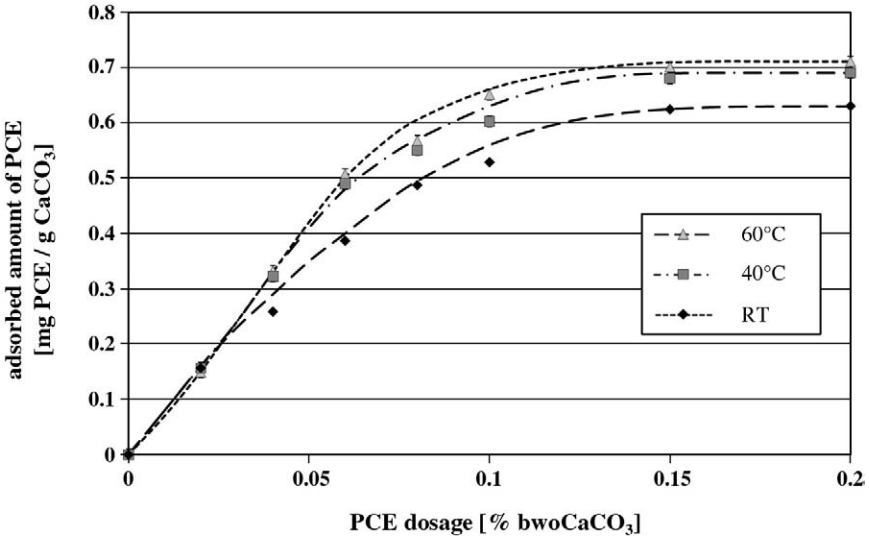

Fig. 10. Adsorption isotherms for PCE S23-M19 on $CaCO_3$ at pH 12.6 + 1 g/L Ca^{2+} and RT, 40 °C and 60 °C, resp.

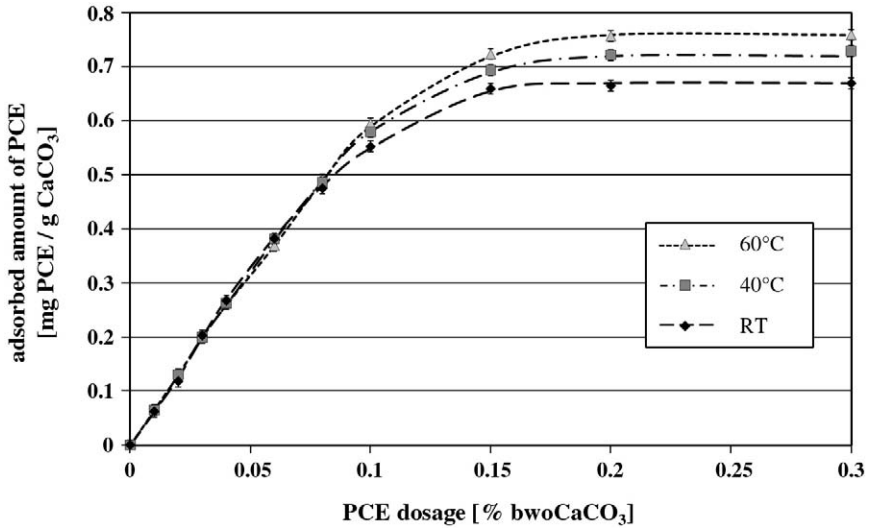

Fig. 11. Adsorption isotherms for PCE S34-M13 on $CaCO_3$ at pH 12.6 + 1 g/L Ca^{2+} and RT, 40 °C and 60 °C, resp.

Generally, the PCE dosages at which the saturated adsorbed amounts are reached increase with increasing side chain length of PCE. This means that for PCEs possessing longer side chains, a higher dosage is required to achieve the maximum load of polymer onto the $CaCO_3$ surface. Further, with increasing temperature, the saturated adsorbed amount of the PCEs possessing short and medium side chain length (S7-M31 and S23-M19) increases whereas for S34-M13, only a minor effect of temperature is observed.

The strongest effect on the saturated adsorbed amount, however, is owed to the presence of Ca^{2+}. For each polymer and independent of the temperature, the saturated adsorbed amount increases by about 100% when Ca^{2+} is present. Thus, in the presence of Ca^{2+}, significantly higher amounts of PCE can be loaded onto the $CaCO_3$ surface. In contrast to the strong effect of Ca^{2+}, pH has very little impact. Also, the slope decreases at which the adsorbed amount increases as a function of PCE concentration. Consequently, when Ca^{2+} is present, a higher PCE dosage is necessary to load the same amount of polymer on the surface as in the absence of Ca^{2+}. Both effects are undesirable for the application of PCE superplasticizers, because they increase dosages and cost.

Another interesting observation is that at pH 12.6 where $CaCO_3$ possesses a negative surface charge (zeta potential −12 mV, see Table 3), anionic PCEs can still adsorb, in spite of the electrostatic repulsion (Figs. 6–8). A potential explanation for this unexpected behaviour is that the negative surface charge of $CaCO_3$ is the result of OH^- adsorption onto the initially positively charged surface. When PCE is added, these adsorbed OH^- anions are released into the pore solution whereas PCE takes their sites on the $CaCO_3$ surface.

For each PCE and in three different pore solutions, ΔG_0, ΔH_0 and ΔS_0 were determined following the method described by BOUHAMED et al. [1]:

At first, a linear LANGMUIR regression was made for each temperature and PCE by plotting the equilibrium concentrations of non-adsorbed PCE (C_{eq}) which was obtained by TOC measurement against the quotient of non-adsorbed to adsorbed PCE (C_{eq}/Q_{ads}). Q_{ads} were taken from the adsorption isotherms shown in Figs. 3–11 and converted into mol/L units. As an example, for S7-M31 the resulting three LANGMUIR regression lines each representing a different temperature are shown in Fig. 12. The error is indicated by bars.

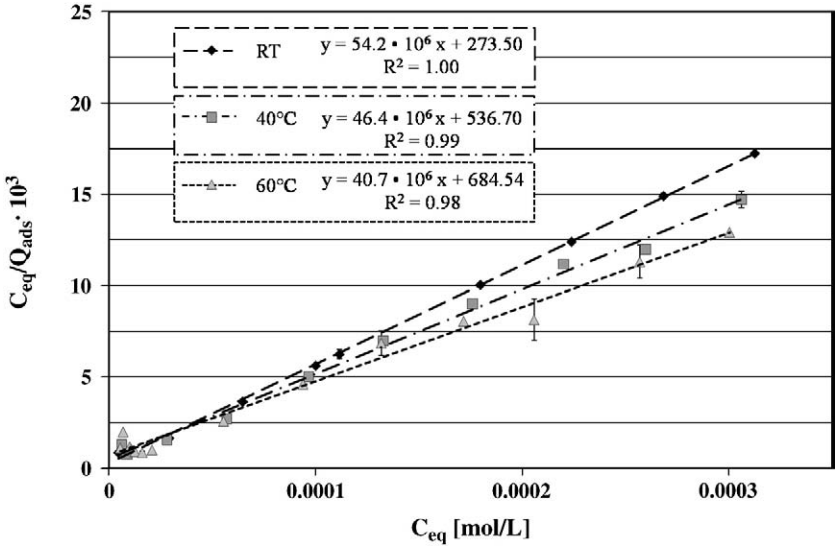

Fig. 12. Linear LANGMUIR regression of the adsorption isotherms of PCE S7-M31 on $CaCO_3$ at pH 9 and RT, 40 °C and 60 °C, resp.

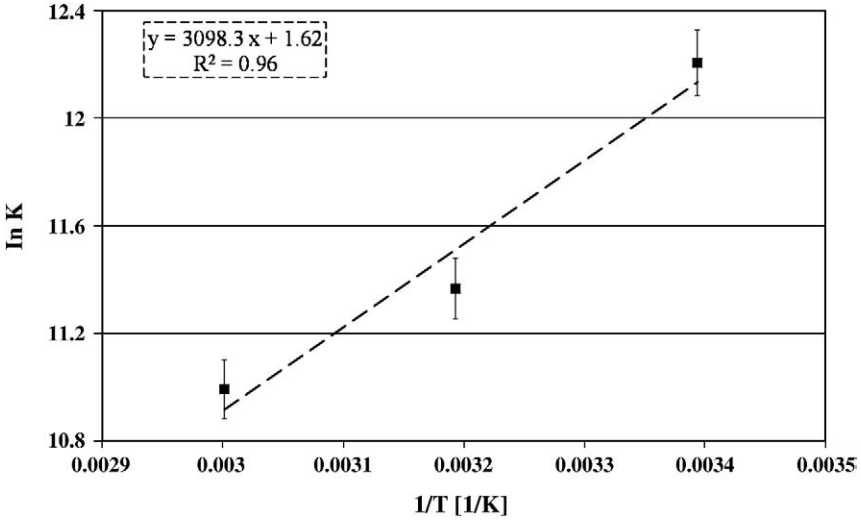

Fig. 13. VAN'T HOFF plot of the temperature dependence of the adsorption equilibrium constant K for PCE S7-M31 on $CaCO_3$ at pH 9.

Next, the temperature dependent adsorption equilibrium constant K was determined according to Eq. (5) which derives from Eq. (2). Q_{max} is the reciprocal of the slope of the regression lines shown in Fig. 12, and f represents the intercept of the regression line with the (C_{eq}/Q_{ads}) axis.

$$K = \frac{1}{Q_{max} \cdot f} \tag{5}$$

As an example, the calculation of K for S7-M31 at RT is shown: according to Fig. 12, at room temperature the slope of the regression line is $54.2 \cdot 10^6$. With f being 273.50 (Fig. 12), the K value for S7-M31 at RT and pH 9 is $K(\text{S7-M31})_{\text{RT, pH 9}} = (54.2 \cdot 10^6) : 273.50 = 2.0 \cdot 10^5$.

By plotting $1/T$ against ln K (= VAN'T HOFF plot), a regression line is obtained in which the slope is $-\Delta H_0/R$ and the intercept with the y-axis is $\Delta S_0/R$ (see Eq. (3)). Thus, for S7-M31 at pH 9 (Fig. 13), ΔH_0 is calculated as follows: $\Delta H_0\ (\text{S7-M31})_{\text{pH 9}} = -\text{slope} \cdot R = -3.10 \cdot 10^3 \cdot 8.314$ [J/mol] = −25.8 [kJ/mol]. All ΔH_0 values characteristic for the adsorption of PCEs in three different pore solutions were calculated in this manner and are shown in Tables 4–6.

Next, the standard entropy of adsorption ΔS_0 was calculated by multiplying the value of the intercept point between the regression line and the y-axis (Fig. 13) with R. Again, as an example, the calculation of ΔS_0 for S7-M31 at pH 9 is shown: $\Delta S_0\ (\text{S7-M31})_{\text{pH 9}} = 1.62 \cdot 8.314$ [J/mol K] = +13.5 [J/mol K]. All ΔS_0 values shown for the PCEs in Tables 4–6 were calculated following this principle method.

Finally, ΔG_0 values were calculated according to the GIBBS–HELMHOLTZ equation $\Delta G_0 = \Delta H_0 - T \cdot \Delta S_0$, where $T = 294.65$ K (21.5 °C). It becomes apparent that for all polymers tested, a decreased enthalpic contribution resulting from a lower anionic charge of the PCE as a consequence of increased side chain length is compensated by a higher entropic contribution. This way, the ΔG_0 values for all three PCE polymers are quite comparable when studied in the same pore solution. There is, however, a clear tendency for a decrease in ΔG_0 in the Ca^{2+} loaded pore solution (~−26 kJ/mol), compared with the two other pore solutions ($\Delta G_0 \sim -30$ kJ/mol).

Following is a discussion of the thermodynamic values shown in Tables 4–6 and the factors which influence them. The portion of enthalpic and entropic contribution to the adsorption process of each PCE will be compared.

3.3.1. Influence of PCE architecture

The exothermic character of ΔH_0 generally decreases in the order S7-M31 → S23-M19 → S34-M13, no matter which pH or Ca^{2+} concentration exists in the pore solution. Obviously, ΔH_0 correlates well with the length of the PCE side chain. Longer side chains result in lower values for the enthalpy of adsorption. At the same time, longer side chains produce higher entropy gains. Consequently, the adsorption of PCEs possessing short side chains mainly occurs for enthalpic reasons. Whereas, the driving force behind the adsorption of PCEs with long side chains is a substantial gain in entropy.

3.3.2. Influence of pH

Increase of pH from 9 to 12.6 results in an increase of ΔS_0 (entropy gain) which is almost compensated by lower ΔH_0 values (Tables 4 and 5). As a result, the ΔG_0 values are hardly affected by pH. All ΔG_0 values are negative, indicating that adsorption of these PCEs is an exergonic (spontaneous) process which is favoured by a release of energy (exothermic). Surprisingly, at pH 12.6 where $CaCO_3$ shows a negative surface potential, ΔH_0 is only slightly decreased, in spite of the electrostatic repulsion between the anionic polymers and the negatively charged mineral surface. At the same time, an increase in entropy is observed which can be explained by the release of OH^- anions from the $CaCO_3$ surface. This way, the thermodynamic parameters support our theory of a substitution process occurring during adsorption of PCE at pH 12.6.

Table 4
ΔH_0, ΔS_0, $-T \cdot \Delta S_0$ and ΔG_0 values for the adsorption of different PCEs on $CaCO_3$ at pH 9 and room temperature.

PCE	ΔH_0 (kJ/mol)	ΔS_0 (J/mol K)	$-T \cdot \Delta S_0$ (kJ/mol)	ΔG_0 (kJ/mol)
S7-M31	−25.8 ± 0.3	+13.5 ± 1.7	−4.0 ± 0.5	−29.8 ± 0.8
S23-M19	−21.2 ± 1.8	+34.1 ± 3.2	−10.1 ± 0.9	−31.3 ± 2.7
S34-M13	−18.3 ± 2.0	+38.4 ± 7.0	−11.4 ± 2.1	−29.7 ± 4.1

Table 5
ΔH_0, ΔS_0, $-T \cdot \Delta S_0$ and ΔG_0 values for the adsorption of different PCEs on $CaCO_3$ at pH 12.6 and room temperature.

PCE	ΔH_0 (kJ/mol)	ΔS_0 (J/mol K)	$-T \cdot \Delta S_0$ (kJ/mol)	ΔG_0 (kJ/mol)
S7-M31	−23.2 ± 0.4	+25.3 ± 1.5	−7.5 ± 0.4	−30.7 ± 0.8
S23-M19	−15.9 ± 0.5	+46.6 ± 1.6	−13.8 ± 0.5	−29.7 ± 1.0
S34-M13	−3.7 ± 0.9	+80.9 ± 2.7	−23.8 ± 0.8	−27.5 ± 1.7

Table 6
ΔH_0, ΔS_0, $-T \cdot \Delta S_0$ and ΔG_0 values for the adsorption of different PCEs on $CaCO_3$ at pH 12.6 + 1 g/L Ca^{2+} and room temperature.

PCE	ΔH_0 (kJ/mol)	ΔS_0 (J/mol K)	$-T \cdot \Delta S_0$ (kJ/mol)	ΔG_0 (kJ/mol)
S7-M31	−15.2 ± 1.4	+37.2 ± 4.7	−11.0 ± 1.4	−26.2 ± 2.8
S23-M19	+12.7 ± 1.0	+133.3 ± 4.0	−39.3 ± 1.2	−26.6 ± 2.2
S34-M13	+3.3 ± 1.1	+95.7 ± 3.6	−28.2 ± 1.1	−24.9 ± 2.2

3.3.3. Influence of calcium ions

In the presence of Ca^{2+}, the enthalpic contribution (ΔH_0) to the adsorption decreases dramatically (Table 6). Main reason is the reduction in anionic charge densities of the PCEs owed to calcium complexation (see Table 2). Electrostatic attraction of the PCE molecules to the positively charged $CaCO_3$ surface is much less or there is even an electrostatic repulsion, indicated by slightly positive ΔH_0 values (S23-M19 and S34-M13). Fortunately, this negative effect is more than compensated by a high gain in entropy. This way it is demonstrated that in the presence of Ca^{2+}, PCE adsorption on the $CaCO_3$ surface is almost completely driven by the entropic contribution to the GIBBS free energy. The values of ΔG_0 in the Ca^{2+} loaded solution indicate that the presence of Ca^{2+} generally reduces the tendency of PCE to adsorb onto the $CaCO_3$ surface.

3.3.4. Influence of the surface loading with PCE

Measurements based on the VAN'T HOFF plot do not take into account that the thermodynamic parameters ΔH and ΔS will change during the adsorption process. For example, at the beginning of adsorption, electrostatic attraction between PCE and the surface is maximum. With increasing amount of PCE adsorbed, the surface charge is more and more neutralized. Consequently, the attractive force between PCE and the surface which is expressed by the enthalpy term decreases. Therefore, it is important to study the thermodynamic parameters under different surface loadings. For this reason, we determined the isosteric values (values at constant adsorbed amounts of PCE) of ΔG, ΔH and ΔS according to the method described by HELMY et al. [3].

In the following, calculation of the isosteric enthalpy, entropy and the GIBBS free energy of adsorption based on experimental data for polymer S7-M31 at pH 9 is shown as an example: At first, $\Delta H_{isosteric}$ is determined following the modified CLAUSIUS–CLAPEYRON equation (Eq. (4)). For this purpose, the adsorbed amount of PCE at equilibrium (Q_{ads}) is plotted against ln C_{eq} for three temperatures. The resulting points were fitted with a polynomial approximation curve of the second order. For example, for PCE S7-M31 at pH 9 and RT, the function $y = -0.02x^2 - 0.34x - 1.25$ was obtained as shown in Fig. 14. For each adsorbed amount of PCE, the error bars are displayed in the graph. They show that at 60 °C, the experimental error is considerably higher than at 40 °C and RT, resp. Next, temperature dependent ln $(C_{eq})_{isosteric}$ was obtained by selecting specific surface loadings with polymer (0.05; 0.10; 0.15; 0.20 and 0.25 mg PCE/g $CaCO_3$ from Fig. 14) and inserting these values into the polynomial function. For example, at a surface loading of 0.1 mg/g $CaCO_3$ and RT, the calculation produces the equation $0.1 = -0.02\,x^2 - 0.34x - 1.25$.

Solving this equation for x produces $x = -12.21$.

Following this method, ln $(C_{eq})_{isosteric}$ values presenting different surface loadings at different temperatures were calculated and plotted against $1/T$, as is shown in Fig. 15. There, the relative error is extremely small.

$\Delta H_{isosteric}$ is obtained by multiplying the slope of the lines shown in Fig. 15 with R. As an example, for a surface loading of 0.1 mg S7-M31/g $CaCO_3$ at pH 9, the slope is −898 (Fig. 15). Thus, $\Delta H_{isosteric}$ is $-898 \cdot 8.314$ [J/mol] = −7.5 kJ/mol.

$\Delta S_{isosteric}$ is obtained by multiplying the intercept point of the straight line with the y-axis in Fig. 15 ($\ln(C_{eq})_{isosteric}$) with $-R$ (Eq. (3)). For example, for a surface loading with 0.1 mg S7-M31/g $CaCO_3$ at pH 9, $\Delta S_{isosteric}$ is $-9.16 \cdot (-R) = -9.16 \cdot (-8.314)$ [J/mol K] = +76.2 [J/mol K].

Finally, $\Delta G_{isosteric}$ is calculated from the $\Delta H_{isosteric}$ and $\Delta S_{isosteric}$ values according to the GIBBS–HELMHOLTZ equation (Eq. (1)). The values obtained for the isosteric ΔG, ΔH and $-T \cdot \Delta S$ at different surface loadings of S7-M31 are displayed in Fig. 16. As can be seen there, the relative error for each thermodynamic parameter is quite small. The result allows to conclude as follows:

For PCE S7-M31 in $CaCO_3$ suspension at pH 9, the isosteric GIBBS free energy of adsorption decreases with increasing surface loading of the substrate with PCE. At low surface loading, the adsorption process is driven by both enthalpic ($\Delta H < 0$) and entropic ($\Delta S > 0$) contributions. The adsorbed PCE macromolecule represents an energetically more favourable state than the dissolved one. With increasing surface loading, however, the enthalpic contribution to the GIBBS free energy of adsorption decreases and the entropic contribution increases. Such an opposite development of enthalpic and entropic contributions has been reported already for hydrolyzed polyacrylnitrile interacting with cellulose [11]. At very high surface loadings, the entire adsorption process becomes endothermic and stops. The reason is that electrostatic repulsion between PCE molecules within the adsorbed polymer layer and steric repulsion between adsorbed and non-adsorbed PCE macromolecules existing in solution becomes prevalent at high surface loadings.

This effect can be explained by zeta potential measurements. When PCE S7-M31 is titrated to an aqueous $CaCO_3$ suspension (pH 9), the zeta potential of the initially positively charged $CaCO_3$ surface becomes negative until it reaches a plateau (Fig. 17). At low surface loadings, the macromolecules adsorb onto the positively

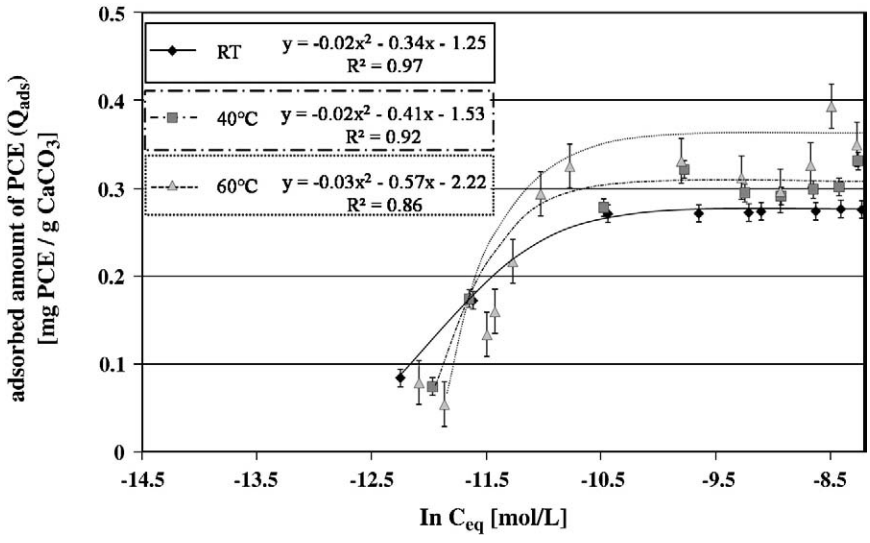

Fig. 14. Polynomial approximation of the function $Q_{ads} = f(\ln C_{eq})$ for PCE S7-M31 on $CaCO_3$ at pH 9 and RT, 40 °C and 40 °C, resp.

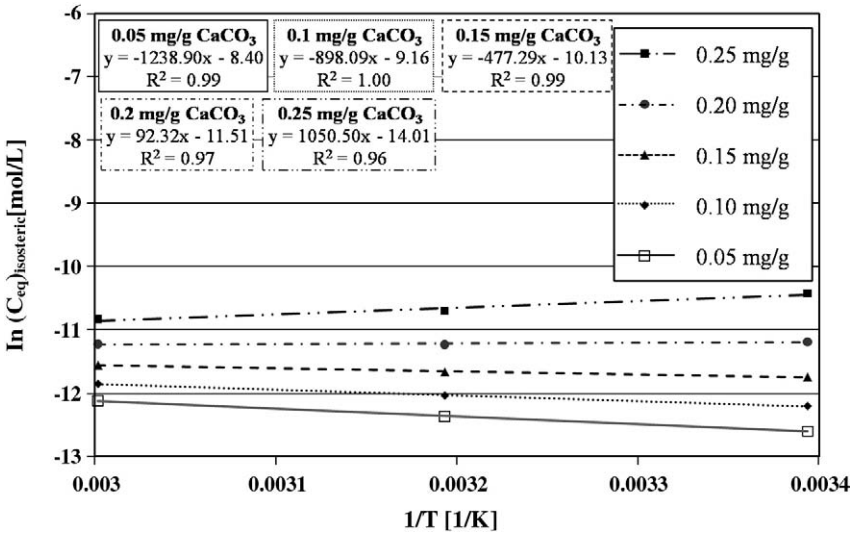

Fig. 15. CLAUSIUS–CLAPEYRON plots for different surface loadings of PCE S7-M31 on $CaCO_3$ at pH 9.

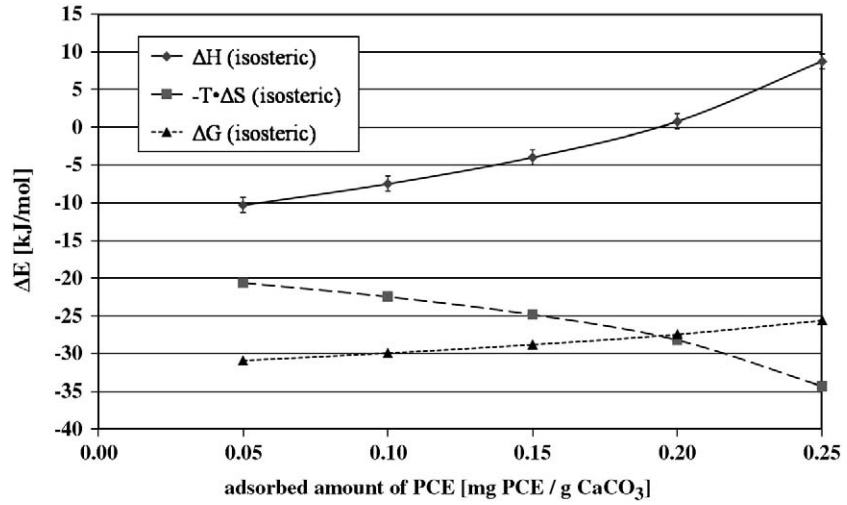

Fig. 16. $\Delta H_{(\text{isosteric})}$, $-T\cdot\Delta S_{(\text{isosteric})}$ and $\Delta G_{(\text{isosteric})}$ at RT as a function of amount of PCE S7-M31 adsorbed on $CaCO_3$ at pH 9 and room temperature.

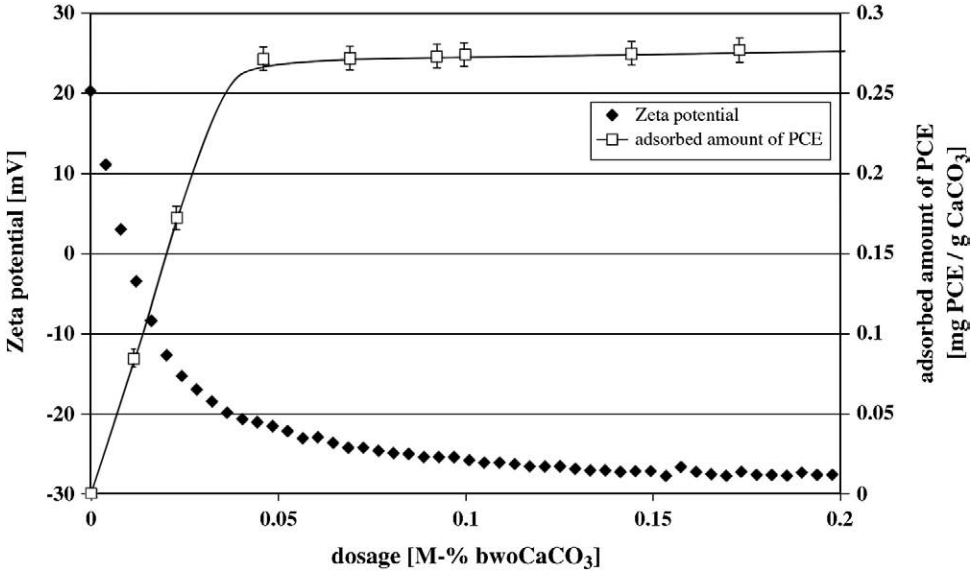

Fig. 17. Zeta potential of an aqueous $CaCO_3$ suspension (pH 9) and adsorption isotherm for PCE S7-M31 as a function of PCE dosage (RT; $w/b = 0.425$).

charged $CaCO_3$ surface via strong electrostatic attraction and an increase in entropy. The adsorption process is exothermic. At high surface loadings, the zeta potential of the $CaCO_3$ surface becomes negative in sign. The electrostatic attraction between PCE and the surface becomes weaker and finally turns into repulsion. From the point of enthalpy, the adsorption process has then become endothermic. Nevertheless, adsorption still proceeds spontaneously to higher surface loadings. The reason is a continuous gain in entropy resulting from the release of a huge amount of water molecules adsorbed on the inorganic surface and the polymer. The water molecules coordinating atoms on the surface of $CaCO_3$ will be released by the adsorption of PCE macromolecules [12]. Additionally, it is to be expected that in the adsorbed state, some of the water molecules bound to the carboxylate groups and the polyethylene oxide side chains of the polycarboxylate will be released as well. This way, adsorption of PCE even at high surface loadings is explained by a huge gain in entropy resulting from the loss of the hydrate shell within the polymer layer due to polymer–polymer interactions.

4. Conclusions

The adsorption of PCE superplasticizers on limestone in aqueous suspension is a complex process. Energetically, it is driven by an enthalpic contribution resulting from the electrostatic attraction between the opposite charges of substrate and PCE ($\Delta H<0$), and an entropic contribution which derives from the release of numerous counter ions and water molecules into the pore solution ($\Delta S>0$). The enthalpic and entropic contributions to the GIBBS free energy of adsorption depend on the ionic composition of the pore solution, on the molecular architecture of the PCE molecule, its molecular weight and types of anchor groups and on the surface loading of the substrate with PCE. Generally, the adsorption process is less exothermic and therefore less favoured in the presence of Ca^{2+} ions. This effect can be explained by the Ca^{2+} complexation of the carboxylate groups which results in a lower anionic charge density of the PCE molecules. Thus, electrostatic attraction (ΔH) between the substrate and the PCE molecules decreases. Contrary to this is a high gain in entropy in the presence of Ca^{2+} ions, resulting from PCE adsorption.

As expected, the thermodynamic parameters describing the adsorption process also depend on the molecular architecture of the PCEs. The anionic charge density of a PCE influences both enthalpy and entropy. The higher the anionic charge density, the higher is the enthalpic contribution to adsorption. The entropic contribution increases with lower anionic charge density resulting from increasing side chain length of the PCE macromolecule.

The thermodynamic parameters also depend on the surface loading of the substrate with polymer. For a PCE with short side chains and low surface loadings, adsorption is exothermic, mainly through electrostatic attraction between the opposite charges of substrate and polymer. With increasing surface loading, electrostatic repulsion between the adsorbed polymer layer and solved PCE molecules approaching the surface becomes more prevalent. This way, the adsorption process becomes endothermic at high surface loadings and comes to a halt.

The results of this work describe the principle forces driving the adsorption of PCE superplasticizers on inorganic surfaces. The findings demonstrate that, besides electrostatic attraction between the polymer and the inorganic surface, a gain in entropy is the major force driving PCE adsorption. In cement paste, the entropy effect is particularly pronounced, because there, many PCEs exhibit low or nearly zero anionic charge densities which result in low ΔH_0 values. The results from this study indicate that in cementitious systems such as e.g. concrete, superplasticizer molecules which achieve a particularly high gain in entropy will adsorb in higher amounts and may represent more effective superplasticizers.

References

[1] H. Bouhamed, S. Boufi, A. Magnin, Dispersion of alumina suspension using comb-like and diblock copolymers produced by RAFT polymerization of AMPS and MPEG, J. Colloid Interf. Sci. 312 (2007) 279–291.
[2] Z. Rawajfih, N. Nsour, Thermodynamic analysis of sorption isotherms of chromium (VI) anionic species on reed biomass, J. Chem. Thermodyn. 40 (2008) 846–851.
[3] K. Helmy, E. Ferreiro, S. De Bussetti, Energy, enthalpy, and isosteric heat of adsorption of phosphate on hydrous Al oxide, J. Colloid Interf. Sci. 183 (1996) 131–134.
[4] E. Sakai, A. Kawakami, M. Daimon, Dispersion mechanisms of comb-type superplasticizers containing grafted poly(ethylene oxide) chains, Macromol. Symp. 175 (2001) 367–376.
[5] O. Blask, D. Honert, The electrostatic potential of highly filled cement suspensions containing various superplasticizers, Seventh CANMET/ACI International Conference on Superplasticizers and Other Chemical Admixtures in Concrete SP-217, 2003, pp. 87–101.
[6] K. Yoshioka, E. Tazawa, K. Kawai, T. Enohata, Adsorption characteristics of superplasticizers on cement component minerals, Cem. Concr. Res. 32 (2002) 1507–1513.
[7] J. Plank, B. Sachsenhauser, Impact of molecular structure on zeta potential and adsorbed conformation of α-allyl-ω-methoxypolyethylene glycol-maleic anhydride superplasticizers, J. Adv. Concr. Technol. 4 (2) (2006) 233–239.
[8] J. Plank, B. Sachsenhauser, Experimental determination of the effective anionic charge density of polycarboxylate superplasticizers in cement pore solution, Cem. Concr. Res. 39 (2009) 1–5.
[9] J. Plank, K. Pöllmann, N. Zouaoui, P. Andres, C. Schaefer, Synthesis and performance of methacrylic ester based polycarboxylate superplasticizers possessing hydroxy terminated poly(ethylene glycol) side chains, Cem. Concr. Res. 38 (2008) 1210–1216.
[10] A. Kaufman Katz, J. Glusker, S. Beebe, C. Bock, Calcium ion coordination: a comparison with that of beryllium, magnesium, and zinc, J. Am. Chem. Soc. 118 (1996) 5752–5763.
[11] M. Nedeltscheva, S. Bencheva, E. Valcheva, V. Valchev, Study of the thermodynamics of adsorption of hydrolyzed modified polyacrylnitrile, Colloid Polym. Sci. 265 (1987) 312–317.
[12] C. Geffroy, A. Foissy, J. Persello, B. Cabane, Surface complexation of calcite by carboxylates in water, J. Colloid Interf. Sci. 211 (1999) 45–53.